Supporting Information

Designed formation of $Co_3O_4/ZnCo_2O_4/CuO$ hollow polyhedral nanocages derived from zeolitic imidazolate framework-67 for high-performance supercapacitors

Saisai Zhou, Zhaochun Ye, Sizhong Hu, Chen Hao*, Xiaohong Wang*, Chengxiang Huang and Fangsheng Wu

School of Chemistry and Chemical Engineering, Jiangsu University, Zhenjiang, Jiangsu 212013, China

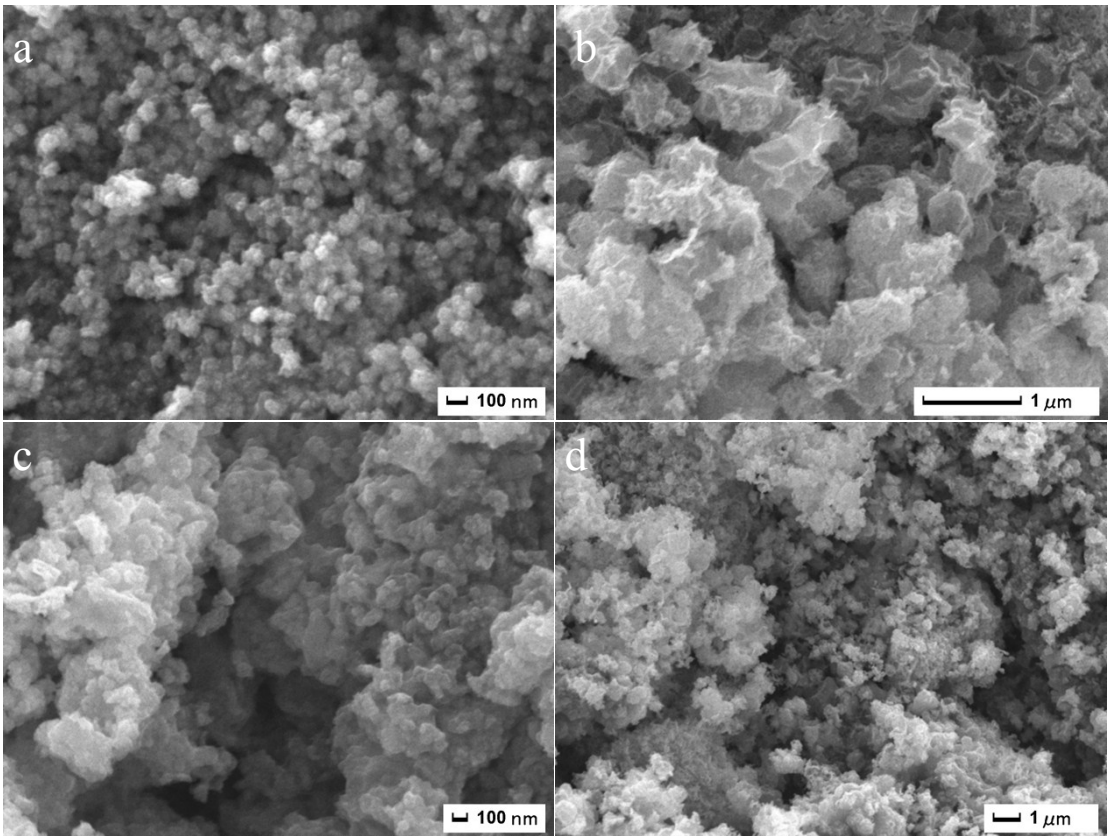

Fig. S1 SEM images of $Co_3O_4/ZnCo_2O_4/CuO$-2 HPNCs (a,b) and $Co_3O_4/ZnCo_2O_4/CuO$-3(c,d).

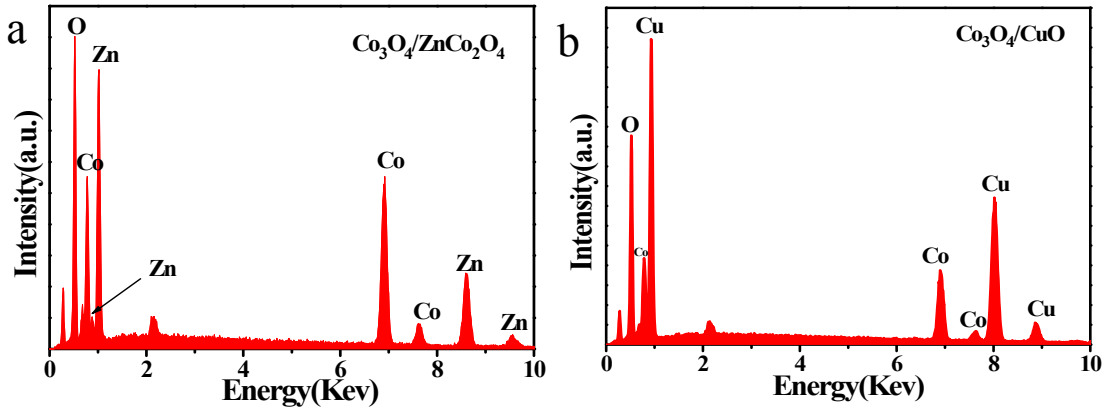

Fig. S2 The Energy-dispersive spectroscopy (EDS) of (a) $Co_3O_4/ZnCo_2O_4$ HPNCs and (b) Co_3O_4/CuO HPNCs.

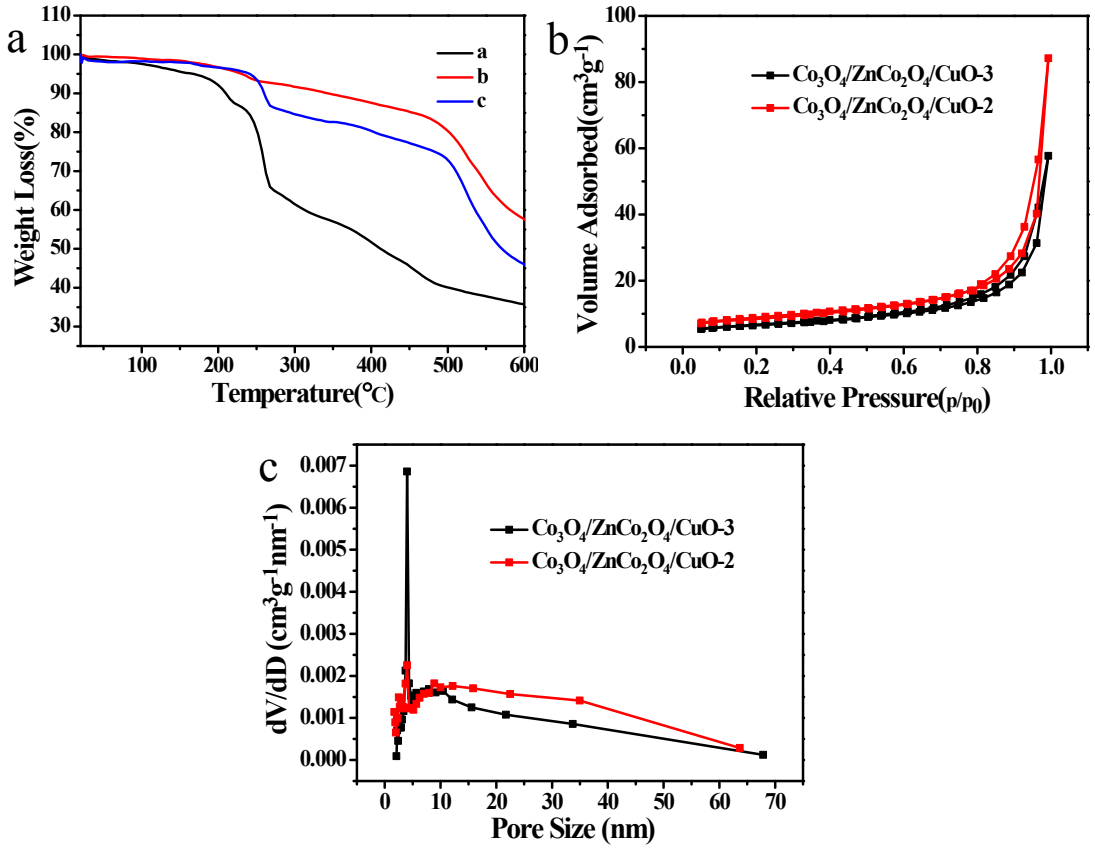

Fig. S3 (a) TGA curves of a: Co_3O_4/CuO; b: Co_3O_4/$ZnCo_2O_4$; c: Co_3O_4/$ZnCo_2O_4$/CuO-1; (b) N_2 adsorption-desorption isotherm curves and (c) the pore size distribution curves of Co_3O_4/$ZnCo_2O_4$/CuO-2 HPNCs and Co_3O_4/$ZnCo_2O_4$/CuO-3 HPNCs.

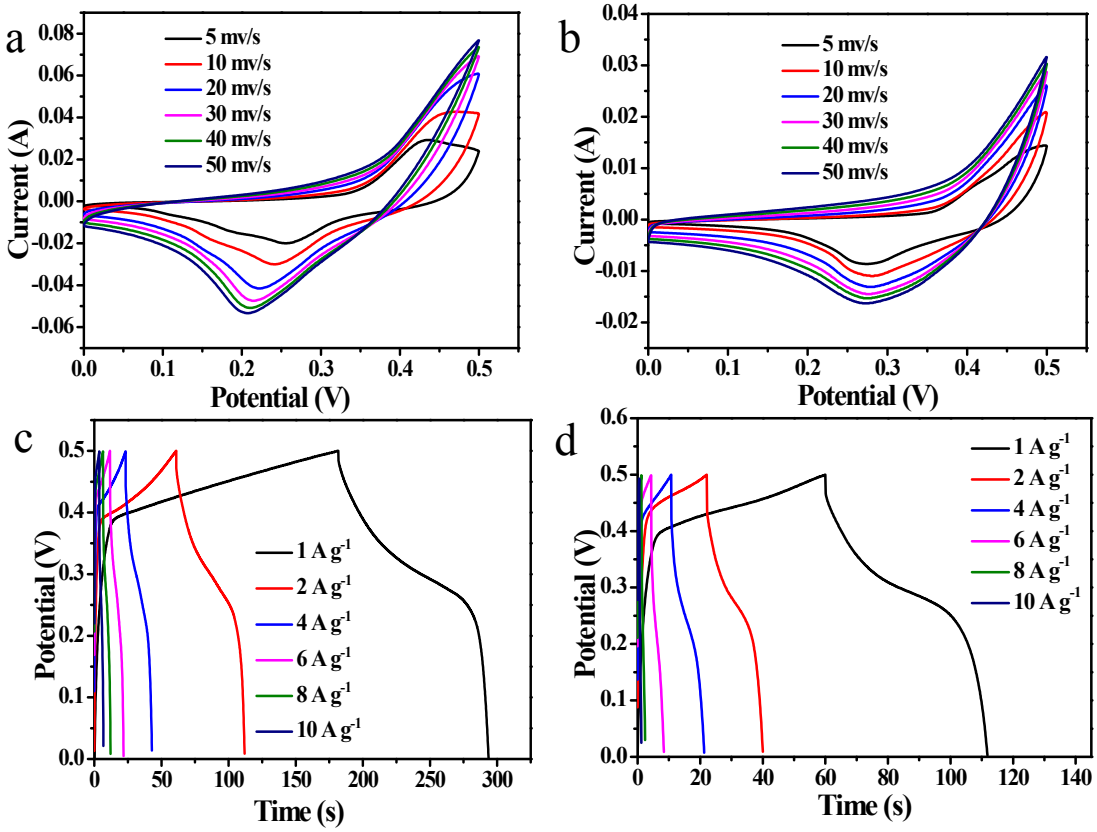

Fig. S4 (a) CV curves of $Co_3O_4/ZnCo_2O_4$ at different scan rates, (b) CV curves of Co_3O_4/CuO at different scan rates, (c) GCD curves of $Co_3O_4/ZnCo_2O_4$ at different current densities, (d) GCD curves of Co_3O_4/CuO at different current densities.

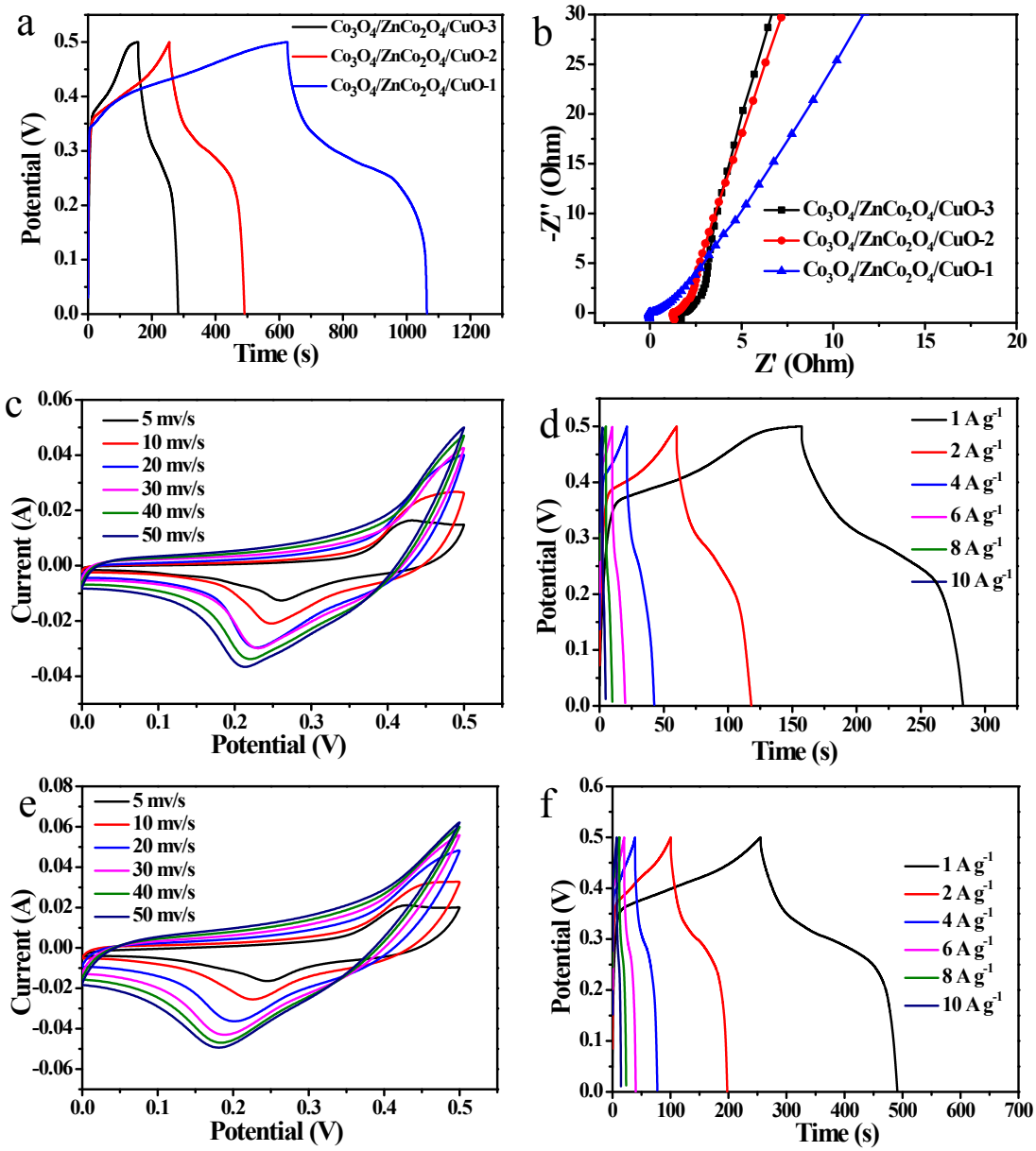

Fig. S5 (a) GCD curves of the composites at a current density of 1 A g^{-1}, (b) Nyquist impedance plots of composites, (c) CV curves of $Co_3O_4/ZnCo_2O_4/CuO$-3 at different scan rates, (d) GCD curves of $Co_3O_4/ZnCo_2O_4/CuO$-3 at different current densities, (e) CV curves of $Co_3O_4/ZnCo_2O_4/CuO$-2 at different scan rates, (f) GCD curves of $Co_3O_4/ZnCo_2O_4/CuO$-2 at different current densities.

As shown in Fig. S5a, it can be seen that the $Co_3O_4/ZnCo_2O_4/CuO$-1 has the longest discharge time at a current density of 1 A g^{-1}, and it indicates that $Co_3O_4/ZnCo_2O_4/CuO$-1 has a larger specific capacitance, which are consistent with the measured results of cyclic voltammetry. The CV curves of $Co_3O_4/ZnCo_2O_4/CuO$-3 and $Co_3O_4/ZnCo_2O_4/CuO$-2 are shown in Fig. S5c and Fig. S5e, respectively. It can be seen that the two electrode materials have the obvious redox peaks in the 0-0.5 V

range of the voltage window, which confirmed the pseudo-capacitance characteristics of the electrode material. The Nyquist plots of the electrodes are shown in Fig. S5b. All the EIS spectra are consisted of one semicircle in the high frequency region and a straight line in the low frequency region. About the three electrodes, the R_s values of $Co_3O_4/ZnCo_2O_4/CuO$-1 is smallest compared with the other two electrodes, indicating that the electrode has a lower solution resistance and Faradaic resistance.

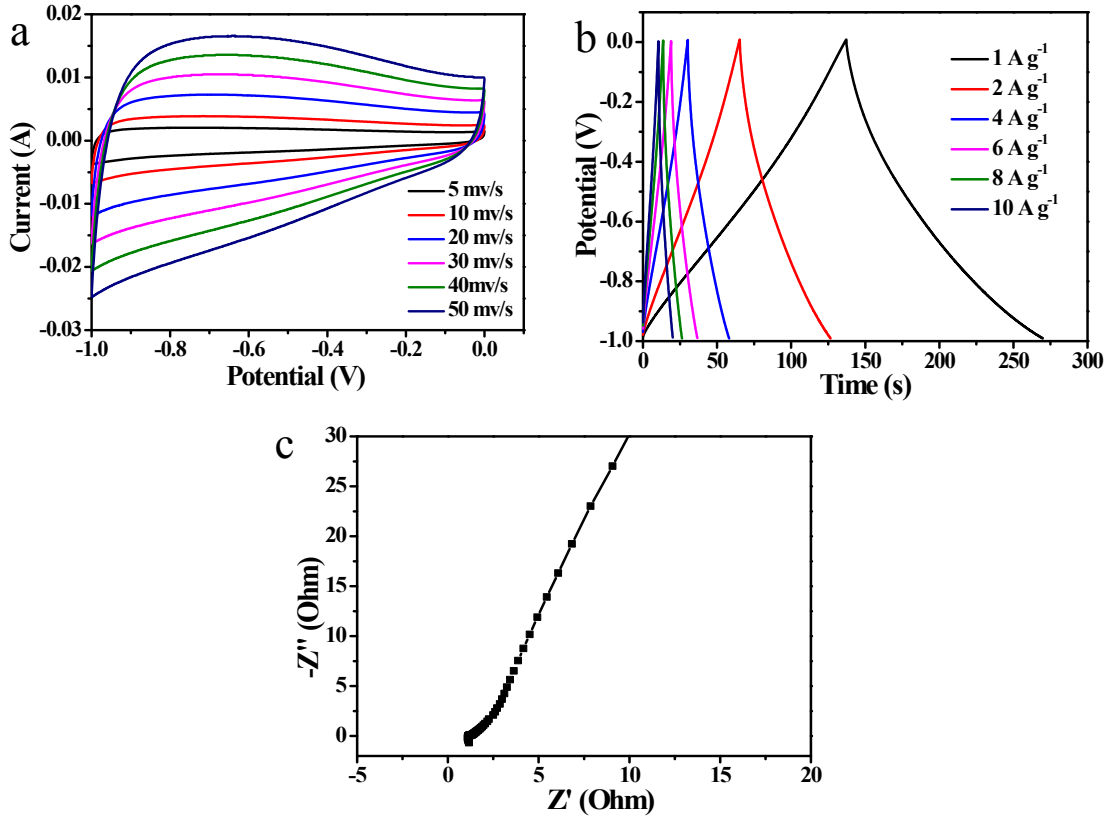

Fig. S6 (a) CV curves of AC at different scan rates, (d) GCD curves of AC at different current densities, (e) Nyquist impedance plots of AC.

Fig. S6a is the CV curves of activated carbon (AC) at different scan rates of 5-50 mV s^{-1}, showing evident quasi-rectangular shape, which indicates that it has good reversible charge-discharge performance in the voltage range of -1.0-0 V. Fig. S6b shows the galvanostatic charge-discharge curves of the activated carbon at the current densities of 1-10 A g^{-1}. These curves are symmetrical and express a almost symmetrical triangle shape. The discharge time decreases gradually with the current

density increasing, and the corresponding capacitance is 133.6, 123.4, 112, 106.2, 101.6, and 97 F g^{-1}, respectively. All these demonstrate the capacitive behaviour of the activated carbon.